Inorg. Chem. **2005**, *44*, 9667–9675

Luminescence Ranging from Red to Blue: A Series of Copper(I)–Halide Complexes Having Rhombic $\{Cu_2(\mu\text{-}X)_2\}$ (X = Br and I) Units with *N*-Heteroaromatic Ligands

Hiromi Araki, Kiyoshi Tsuge,* Yoichi Sasaki,* Shoji Ishizaka, and Noboru Kitamura

Division of Chemistry, Graduate School of Science, Hokkaido University, Sapporo 060-0810, Japan

Received June 23, 2005

A series of Cu(I) complexes formulated as $[Cu_2(\mu\text{-}X)_2(PPh_3)(L)_n]$ were prepared with various mono- and bidentate *N*-heteroaromatic ligands (X = Br, I; L = 4,4′-bipyridine, pyrazine, pyrimidine, 1,5-naphthyridine, 1,6-naphthyridine, quinazoline, *N,N*-dimethyl-4-aminopyridine, 3-benzoylpyridine, 4-benzoylpyridine; $n = 1, 2$). Single-crystal structure analyses revealed that all the complexes have planar $\{Cu_2X_2\}$ units. Whereas those with monodentate *N*-heteroaromatic ligands afforded discrete dinuclear complexes, bidentate ligands formed infinite chain complexes with the ligands bridging the dimeric units. The long Cu···Cu distances (2.872–3.303 Å) observed in these complexes indicated no substantial interaction between the two Cu(I) ions. The complexes showed strong emission at room temperature as well as at 80 K in the solid state. The emission spectra and lifetimes in the microsecond range were measured at room temperature and at 80 K. The emissions of the complexes varied from red to blue by the systematic selection of the *N*-heteroaromatic ligands (λ^{em}_{max}: 450 nm (L = *N,N*-dimethyl-4-aminopyridine) to 707 nm (L = pyrazine)), and were assigned to metal-to-ligand charge-transfer (MLCT) excited states with some mixing of the halide-to-ligand (XL) CT characters. The emission energies were successfully correlated with the reduction potentials of the coordinated *N*-heteroaromatic ligands, which were estimated by applying a simple modification based on the calculated stabilization energies of the ligands by protonation.

Introduction

Recently, there has been considerable interest in the luminescent properties of transition-metal complexes, particularly in view of their potential applications as sensors and light emitting diodes and in artificial photosynthesis.[1−3] Ruthenium(II) and Pt(II) complexes with polypyridyl ligands are representative, and have been investigated from various viewpoints.[4,5] The coinage metal ions with the d^{10} electron configuration are known to afford emissive complexes. Gold(I) complexes have been extensively studied because of their strong emission and interesting photophysical properties related to aurophilicity.[6] Copper(I) complexes, which are inexpensive, abundant, and as strongly emissive as d^{10} Au(I) complexes, have received increased attention.[6e,7] Bis-1,10-phenanthroline(phen)−Cu(I) analogues with substituted

* To whom correspondence should be addressed. E-mail: tsuge@sci.hokudai.ac.jp (K.T.), ysasaki@sci.hokudai.ac.jp (Y.S.).

(1) Ward, M. D., Ed. *Comprehensive Coordination Chemistry II: Applications of Coordination Chemistry*; Elsevier: Oxford, U.K., 2004; Vol. 9.
(2) Roundhill, D. M. *Photochemistry and Photophysics of Metal Complexes*; Plenum Press: New York, 1994.
(3) Balzani, V.; Juris, A.; Venturi, M.; Campagna, S.; Serroni, S. *Chem. Rev.* **1996**, *96*, 759−834.
(4) (a) Dürr, H.; Bossmann, S. *Acc. Chem. Res.* **2001**, *34*, 905−917. (b) Serroni, S.; Campagna, S.; Puntoriero, F.; Loiseau, F.; Ricevuto, V.; Passalacqua, R.; Galletta, M. *C. R. Chim.* **2003**, *6*, 883−893. (c) Balzani, V.; Juris, A. *Coord. Chem. Rev.* **2001**, *211*, 97−115. (d) Bignozzi, C. A.; Argazzi, R.; Kleverlaan, C. J. *Chem. Soc. Rev.* **2000**, *29*, 87−96.
(5) (a) Hissler, M.; McGarrah, J. E.; Connick, W. B.; Geiger, D. K.; Cummings, S. D.; Eisenberg, R. *Coord. Chem. Rev.* **2000**, *208*, 115−137. (b) van Slageren, J.; Klein, A.; Zalis, S. *Coord. Chem. Rev.* **2002**, *230*, 193−211. (c) Demas, J. N.; DeGraff, B. A. *Coord. Chem. Rev.* **2001**, *211*, 317−351.
(6) Some selected references: (a) Vogler, A.; Kunkely, H. *Coord. Chem. Rev.* **2001**, *219−221*, 489−507. (b) Zhang, H.-X.; Che, C.-M. *Chem.−Eur. J.* **2001**, *7*, 4887−4893. (c) Fu, W.-F.; Chan, K.-C.; Cheung, K.-K.; Che, C.-M. *Chem.−Eur. J.* **2001**, *7*, 4656−4664. (d) White-Morris, R. L.; Olmstead, M. M.; Balch, A. L. *J. Am. Chem. Soc.* **2003**, *125*, 1033−1040. (e) Yam, V. W.-W.; Lo, K. K.-W. *Chem. Soc. Rev.* **1999**, *28*, 323−334. (f) Tzeng, B.-C.; Chan, C.-K.; Cheung, K.-K.; Che, C. M.; Peng, S.-M. *Chem. Commun.* **1997**, 135. (g) Chao, H.-Y.; Lu, W.; Li, Y.; Chan, M. C. W.; Che, C.-M.; Cheung, K.-K.; Zhu, N. *J. Am. Chem. Soc.* **2002**, *124*, 14696−14706.
(7) (a)McMillin, D. R.; McNett, K. M. *Chem. Rev.* **1998**, *98*, 1201−1220. (b) Armaroli, N. *Chem. Soc. Rev.* **2001**, *30*, 113−124.

10.1021/ic0510359 CCC: $30.25
Published on Web 11/16/2005

phen ligands give a strong emission related to the structural rigidity and the π^* level of the ligands.[7,8] In addition to monomeric Cu(I) complexes, several polymeric Cu(I)−halide compounds are known to be emissive.[9] Of these, the characteristic dual emissions observed for a series of tetranuclear complexes $\{Cu_4I_4L_4\}$ (L = py, substituted py) are noteworthy. The emissions have been assigned to XLCT (I−L charge-transfer) and CC (cluster-centered) excited states on the basis of experimental and theoretical studies.[9,10]

The rational synthesis of the complexes with intense emission at desired energies has important practical applications.[11] Whereas colored transition-metal complexes may not be suitable candidates for blue (or green) emissions, monovalent coinage metal ions can afford colorless complexes with emissions over the entire visible region. In the oligomeric Cu(I)−halide family, besides the strongly luminescent $[Cu_4(\mu_3\text{-}X)_4L_4]$ complexes, a number of complexes with the rhombic $\{Cu_2(\mu\text{-}X)_2\}$ dimeric unit have been reported. Although many $\{Cu_2(\mu\text{-}X)_2\}$ complexes with the unit have been structurally characterized by X-ray diffraction,[12] their luminescent properties have been reported in only a few cases. This is in contrast to the tetracopper complexes. Reports on the photophysical properties of complexes with this dinuclear unit are limited to $[Cu_2(\mu\text{-}I)_2(L)_n]$ (L = quinoline,[10f] pyridine (py),[10d] tetraethylethylenediamine (Et_4en)[10d]), $[Cu_2(\mu\text{-}I)_2(PPh_3)_2(L)_n]$ (L = py,[9a] 4,4′-bipyridine[13]), and $[Cu_2(\mu\text{-}X)_2(PPh_3)_2(L)_n]$ (X = Br, L = py;[9a] X = Cl, L = py,[9a,14] pyrazine[14]). The emissive excited states are metal-centered for $[Cu_2(\mu\text{-}I)_2(py)_4]$ and $[Cu_2(\mu\text{-}I)_2(Et_4en)_2]$,[10d] and metal-to-ligand charge transfer (MLCT) or halide-to-ligand CT (XLCT) for $[Cu_2(\mu\text{-}Cl)_2(PPh_3)_2(pyz)]$ and $[Cu_2(\mu\text{-}X)_2(PPh_3)_2(py)_2]$.[9a,14] With the aim of understanding the emissive properties of the $\{Cu_2(\mu\text{-}X)_2\}$ complexes and designing complexes with emissions ranging over the visible region, we have carried out the preparation of the complexes with a $\{Cu_2(\mu\text{-}X)_2\}$ unit with a series of *N*-heteroaromatic ligands. The selective preparation of complexes with $\{Cu_2(\mu\text{-}X)_2\}$ units was difficult because of the coordination lability of Cu(I) ions, particularly in polar organic solvents. By using PPh_3 as a co-ligand, however, we have successfully prepared a series of mixed-ligand complexes $[Cu_2(\mu\text{-}X)_2(PPh_3)_2(L)_n]$ (X = I, Br; L = 4,4′-bipyridine, pyrazine, pyrimidine, 1,5-naphthyridine, 1,6-naphthyridine, quinazoline, *N*,*N*-dimethyl-4-aminopyridine, 3-benzoylpyridine, 4-benzoylpyridine, piperazine; n = 1, 2) as crystalline materials using nine different *N*-heteroaromatic ligands (Chart 1). We demonstrate here that the emissive properties of these complexes can be controlled rationally by the proper choice of *N*-heteroaromatic ligands.

Chart 1. Ligands Used in This Study

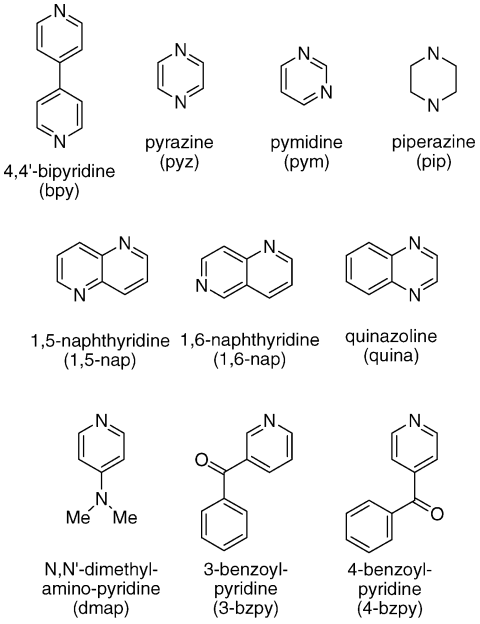

Experimental Section

Reagents. Reagents were purchased from WAKO, Aldrich, and TCI. All reagents were used as received.

Preparation of Complexes. $[Cu_2(\mu\text{-}Br)_2(PPh_3)_2(CH_3CN)_2]\cdot 2CH_3CN$. To an acetonitrile solution of CuBr (150 mg, 1.05 mmol,

(8) (a) Kuang, S.-M.; Cuttell, D. G.; McMillin, D. R.; Fanwick, P. E.; Walton, R. A. *Inorg. Chem.* **2002**, *41*, 3313−3322. (b) Cuttell, D. G.; Kuang, S.-M.; Fanwick, P. E.; McMillin, D. R.; Walton, R. A. *J. Am. Chem. Soc.* **2002**, *124*, 6−7. (c) Cunningham, C. T.; Moore, J. J.; Cunningham, K. L. H.; Fanwick, P. E.; McMillin, D. R. *Inorg. Chem.* **2000**, *39*, 3638−3644. (d) Crane, D. R.; Ford, P. C. *Inorg. Chem.* **1993**, *32*, 2391−2393. (e) Crane, D. R.; Ford, P. C. *J. Am. Chem. Soc.* **1991**, *113*, 8510−8516. (f) Crane, D. R.; DiBenedetto, J.; Palmer, C. E. A.; McMillin, D. R.; Ford, P. C. *Inorg. Chem.* **1988**, *27*, 3698−3700. (g) Dietrich-Buchecker, C. O.; Marnot, P. A.; Sauvage, J. P.; Kirchoff, J. R.; McMillin, D. R. *Chem. Commun.* **1983**, 513−515. (h) McMillin, D. R.; Buckner, M. T.; Ahn, B. T. *Inorg. Chem.* **1977**, *16*, 943

(9) (a) Ford, P. C.; Cariati, E.; Bourassa, J. *Chem. Rev.* **1999**, *99*, 3625−3647. (b) Kutal, C. *Coord. Chem. Rev.* **1990**, *99*, 213−252.

(10) (a)Vitale, M.; Ford, P. C. *Coord. Chem. Rev.* **2001**, *219*−*221*, 3−16. (b) Vitale, M.; Ryu, C. K.; Palke, W. E.; Ford, P. C. *Inorg. Chem.* **1994**, *33*, 561−566. (c) Ford, P. C.; Vogler, A. *Acc. Chem. Res.* **1993**, *26*, 223. (d) Kyle, K. R.; Ryu, C. K.; Ford, P. C.; DiBenedetto, J. A. *J. Am. Chem. Soc.* **1991**, *113*, 2954−2965. (e) Kyle, K. R.; Palke, W. E.; Ford, P. C. *Coord. Chem. Rev.* **1990**, *97*, 35−46. (f) Rath, N. P.; Holt, E. M.; Tanimura, K. *J. Chem. Soc., Dalton Trans.* **1986**, 2303−2310. (g) Ford, P. C. *Coord. Chem. Rev.* **1994**, *132*, 129−140. (h) Dossing, A.; Ryu, C. K.; Kudo, S.; Ford, P. C. *J. Am. Chem. Soc.* **1993**, *115*, 5132−5137. (i) Ryu, C. K.; Vitale, M.; Ford, P. C. *Inorg. Chem.* **1993**, *32*, 869−874. (j) Vitale, M.; Palke, W. E.; Ford, P. C. *J. Phys. Chem.* **1992**, *96*, 8329−8336.

(11) (a) Ma, B.; Li, J.; Djurovich, P. I.; Yousufuddin, M.; Bau, R.; Thompson, M. E. *J. Am. Chem. Soc.* **2005**, *127*, 28−29. (b) Wang, Q.-M.; Lee, Y.-A.; Crespo, O.; Deaton, J.; Tang, C.; Gysling, H. J.; Gimeno, M. C.; Larraz, C.; Villacampa, M. D.; Laguna, A.; Eisenberg, R. *J. Am. Chem. Soc.* **2004**, *126*, 9488−9489. (c) Lowry, M. S.; Hudson, W. R.; Pascal, R. A., Jr.; Bernhard, S. *J. Am. Chem. Soc.* **2004**, *126*, 14129−14135.

(12) In the CCDC database, more than 200 structures have been reported. For example: (a) Maeyer, J. T.; Johnson, T. J.; Smith, A. K.; Borne, B. D.; Pike, R. D.; Pennington, W. T.; Krawiec, M.; Rheingold, A. L. *Polyhedron* **2003**, *22*, 419−431. (b) Graham, P. M.; Pike, R. D.; Sabat, M.; Bailey, R. D.; Pennington, W. T. *Inorg. Chem.* **2000**, *39*, 5121−5132. (c) Bowmaker, G. A.; Hart, R. D.; Jones, B. E.; Skelton, B. W.; White, A. H. *J. Chem. Soc., Dalton Trans.* **1995**, 3063. (d) Bowmaker, G. A.; Hanna, J. V.; Hart, R. D.; Healy, P. C.; White, A. H. *Aust. J. Chem.* **1994**, *47*, 25. (e) Healy, P. C.; Pakawatchai, C.; White, A. H. *J. Chem. Soc., Dalton Trans.* **1983**, 1917. (f) Dyason, J. C.; Engelhardt, L. M.; Healy, P. C.; Pakawatchai, C.; White, A. H. *Inorg. Chem.* **1985**, *24*, 1950. (g) Hengefeld, A.; Kopf, J.; Nast, R. *Chem. Ber.* **1977**, *110*, 3078. (h) Eller, P. G.; Kubas, G. J.; Ryan, R. R. *Inorg. Chem.* **1977**, *16*, 2454.

(13) Li, R.-Z.; Li, D.; Huang, X.-C.; Qi, Z.-Y.; Chen, X.-M. *Inorg. Chem. Commun.* **2003**, 1017−1019.

(14) Henary, M.; Wootton, J. L.; Khan, S. I.; Zink, J. I. *Inorg. Chem.* **1997**, *36*, 796−801.

60 mL) was added PPh_3 (274 mg, 1.05 mmol) in 40 mL of CH_3CN. Colorless crystals were obtained after a few days in 34% yield (320 mg). Anal. Calcd for $C_{44}H_{42}Br_2Cu_2N_4P_2$: C, 54.16; H, 4.34; N, 5.74. Found: C, 54.23; H, 4.44; N, 5.79.

[{$Cu_2(\mu$-I)$_2$(PPh$_3$)$_2$}(μ-bpy)]$_\infty$ (1-I) (bpy = 4,4′-bipyridine). To a solution of CuI (36 mg, 0.19 mmol) and PPh_3 (99 mg, 0.38 mmol) in DMSO (5 mL) was added bpy (5.9 mg, 0.0038 mmol) to obtain a clear yellow solution. After a few days, **1-I** was obtained as small yellow crystals in 98% yield (32 mg). Anal. Calcd for $C_{46}H_{38}Cu_2I_2N_2P_2$: C, 52.04; H, 3.61; N, 2.64. Found: C, 52.06; H, 3.72; N, 2.40.

[{$Cu_2(\mu$-Br)$_2$(PPh$_3$)$_2$}(μ-bpy)]$_\infty$ (1-Br). To a solution of CuBr (2.9 mg, 0.02 mmol) and PPh_3 (5.8 mg, 0.02 mmol) in DMSO (5 mL) was added bpy (0.65 mg, 0.004 mmol) to obtain a clear yellow solution. After a few days, **1-Br** was obtained as small yellow crystals in 70% yield (2.6 mg). Anal. Calcd for $C_{46}H_{38}Br_2Cu_2N_2P_2$: C, 57.10; H, 3.96; N, 2.89. Found: C, 56.98; H, 4.07; N, 2.79.

{[{$Cu_2(\mu$-I)$_2$(PPh$_3$)$_2$}(μ-pyz)]·2CH$_3$CN}$_\infty$ (2-I·2CH$_3$CN) (pyz = pyrazine). To a solution of CuI (38 mg, 0.20 mmol) and PPh_3 (111 mg, 0.42 mmol) in CH_3CN (30 mL) was added pyz (15.2 mg, 0.20 mmol) to obtain an orange-red solution. After 1 week, **2-I·2CH$_3$CN** was obtained as small red crystals in 40% yield (40 mg). Anal. Calcd for $C_{44}H_{40}Cu_2I_2N_4P_2$: C, 49.14; H, 3.63; N, 4.09. Found: C, 49.15; H, 3.77; N, 4.36. The crystal solvents are slowly released in ambient conditions.

[{$Cu_2(\mu$-Br)$_2$(PPh$_3$)$_2$}(μ-pyz)]$_\infty$ (2-Br). To a solution of CuBr (12.2 mg, 0.085 mmol) and PPh_3 (22.2 mg, 0.08 mmol) in CH_3CN (30 mL) was added pyz (3.4 mg, 0.04 mmol) to obtain an orange-red solution. After 1 week, **2-Br** was obtained as small red crystals in solvated form in 55% yield (19.5 mg). The same compound was also obtained using dichloromethane instead of CH_3CN. The crystal solvents are easily released in ambient conditions. Anal. Calcd for $C_{40}H_{34}Br_2Cu_2N_2P_2$: C, 53.89; H, 3.84; N, 3.14. Found: C, 53.80; H, 3.99; N, 3.06.

[{$Cu_2(\mu$-I)$_2$(PPh$_3$)$_2$}(μ-pym)]$_\infty$ (3-I) (pym = pyrimidine). To the solution of CuI (37 mg, 0.20 mmol) and PPh_3 (108 mg, 0.42 mmol) in CH_3CN (30 mL) was added pym (15.4 μl, 0.20 mmol) to obtain a yellow solution. After 10 days, **3-I** was obtained as small yellow crystals in 25% yield (24 mg). Anal. Calcd for $C_{40}H_{34}Cu_2I_2N_2P_2$: C, 48.75; H, 3.48; N, 2.84. Found: C, 48.71; H, 3.64; N, 2.91.

[{$Cu_2(\mu$-Br)$_2$(PPh$_3$)$_2$}(μ-pym)]$_\infty$ (3-Br). To a solution of CuBr (8.2 mg, 0.06 mmol) and PPh_3 (16.4 mg, 0.06 mmol) in CH_3CN (30 mL) was added pym (9.0 μl, 0.11 mmol) to obtain a yellow solution. After 2 weeks, **3-Br** was obtained as small yellow crystals in 25% yield (11.4 mg). Anal. Calcd for $C_{40}H_{34}Br_2Cu_2N_2P_2$: C, 53.89; H, 3.84; N, 3.14. Found: C, 53.92; H, 3.84; N, 3.18.

[{$Cu_2(\mu$-Br)$_2$(PPh$_3$)$_2$}(μ-1,5-nap)]$_\infty$ (4-Br) (1,5-nap = 1,5-naphthyridine). To a solution of CuBr (5.1 mg, 0.04 mmol) and PPh_3 (10.2 mg, 0.04 mmol) in DMF (15 mL) was added a DMF solution (5 mL) containing 1,5-nap (1.0 mg, 0.008 mmol) to obtain a yellow solution. After 3 days, **4-Br** was obtained as small orange crystals in 16% yield (3.0 mg). Anal. Calcd for $C_{44}H_{36}Br_2Cu_2N_2P_2$: C, 56.12; H, 3.85; N, 2.98. Found: C, 55.97; H, 3.90; N, 2.66.

[{$Cu_2(\mu$-Br)$_2$(PPh$_3$)$_2$}(μ-1,6-nap)]$_\infty$ (5-Br) (1,6-nap: 1,6-naphthyridine). To a solution of CuBr (78.9 mg, 0.55 mmol) and PPh_3 (142.3 mg, 0.54 mmol) in a mixed solvent of CH_2Cl_2 (20 mL) and CH_3CN (10 mL) was added a CH_3CN solution (3 mL) of 1,6-nap (35.8 mg, 0.28 mmol). The orange precipitate that formed was filtered, and then the yellow-orange filtrate was concentrated to 20 mL. After 1 day, the precipitate that deposited was filtered off. The solution afforded orange crystals after two months. Yield 5.5% (14.0 mg). Anal. Calcd for $C_{44}H_{36}Br_2Cu_2N_2P_2$: C, 56.12; H, 3.85; N, 2.98. Found: C, 56.29; H, 4.03; N, 3.00.

[{$Cu_2(\mu$-Br)$_2$(PPh$_3$)$_2$}(μ-quina)]$_\infty$ (6-Br) (quina = quinazoline). To a solution of CuBr (17.1 mg, 0.12 mmol) and PPh_3 (32.8 mg, 0.13 mmol) in CH_3CN (15 mL) was added an aqueous solution (10 mL) of quina (7.9 mg, 0.06 mmol/10 mL) to obtain an orange solution. After 1 day, **6-Br** was obtained as small orange crystals in 35% yield (19.6 mg). Anal. Calcd for $C_{44}H_{36}Br_2Cu_2N_2P_2$: C, 56.12; H, 3.85; N, 2.98. Found: C, 56.13; H, 3.75; N, 3.02.

[Cu$_2$(μ-Br)$_2$(PPh$_3$)$_2$(dmap)$_2$] (7-Br) (dmap = *N*,*N*-dimethyl-4-aminopyridine). To a dichloromethane solution (15 mL) of $[CuBr(PPh_3)(CH_3CN)]_2$ (232.4 mg, 0.26 mmol) was added dmap (62.9 mg, 0.51 mmol) in 5 mL of CH_2Cl_2. After stirring for 2 h, we added 16 mL of hexane to the resulting brown solution to afford the brown precipitate, which was then filtered off. The filtrate gave colorless **7-Br** and blue crystals after a few days. Crystals were isolated by filtration, and the blue crystals were removed by washing with CH_3CN. Yield of the colorless crystals, 9% (23.0 mg). Anal. Calcd for $C_{50}H_{50}Br_2Cu_2N_4P_2$: C, 56.88; H, 4.77; N, 5.31. Found: C, 56.96; H, 4.66; N, 5.28.

[Cu$_2$(μ-Br)$_2$(PPh$_3$)$_2$(3-bzpy)$_2$] (8-Br) (3-bzpy = 3-benzoylpyridine). To a dichloromethane solution (10 mL) of $[CuBr(PPh_3)(CH_3CN)]_2$ (33.8 mg, 0.04 mmol) was added 4-bzpy (13.8 mg, 0.08 mmol) in 0.5 mL of CH_2Cl_2. The resulting yellow solution was concentrated to ca. 2 mL, and a small amount of hexane was added. The complex **8-Br** was obtained as yellow crystals in 78% yield (34.7 mg). Anal. Calcd for $C_{60}H_{48}Br_2Cu_2N_2O_2P_2$: C, 61.18; H, 4.11; N, 2.38. Found: C, 61.04; H, 4.19; N, 2.20.

[Cu$_2$(μ-Br)$_2$(PPh$_3$)$_2$(4-bzpy)$_2$] (9-Br) (4-bzpy = 4-benzoylpyridine). To a dichloromethane solution (20 mL) of $[CuBr(PPh_3)(CH_3CN)]_2$ (32.9 mg, 0.04 mmol) was added 4-bzpy (13.6 mg, 0.07 mmol) in 0.5 mL of CH_2Cl_2. The resulting yellow solution was concentrated to ca. 2 mL, and a small amount of hexane was added. Red crystals of **9-Br** were obtained in 55% yield (24.0 mg). Anal. Calcd for $C_{60}H_{48}Br_2Cu_2N_2O_2P_2$: C, 61.18; H, 4.11; N, 2.38. Found: C, 60.97; H, 4.19; N, 2.23.

{[{$Cu_2(\mu$-I)$_2$(PPh$_3$)$_2$}(pip)]·2CH$_3$CN}$_\infty$ (10-I·2CH$_3$CN) (pip = piperazine). To an acetonitrile solution (15 mL) of CuI (10.1 mg, 0.05 mmol) and PPh_3 (27.8 mg, 0.11 mmol) was added pip (4.1 mg, 0.05 mmol) in 5 mL of CH_3CN. After 1 day, **10-I** was obtained as pale pink crystals in 18% yield (4.5 mg). Anal. Calcd for $C_{40}H_{40}Cu_2I_2N_2P_2$: C, 48.45; H, 4.07; N, 2.83. Found: C, 48.32; H, 4.09; N, 2.74.

[{$Cu_2(\mu$-Br)$_2$(PPh$_3$)$_2$}(pip)]$_\infty$ (10-Br). To an acetonitrile solution (15 mL) of CuBr (7.5 mg, 0.05 mmol) and PPh_3 (27.5 mg, 0.10 mmol) was added pip (4.1 mg, 0.05 mmol) in 5 mL of CH_3CN. After a few days, **10-Br** was obtained as pale pink crystals in 26% yield (5.8 mg). Anal. Calcd for $C_{40}H_{40}Br_2Cu_2N_2P_2$: C, 53.52; H, 4.49; N, 3.12. Found: C, 53.43; H, 4.64; N, 3.10.

Physical Measurements. Emission spectra were measured using a photodiode array detector (Hamamatsu, PMA-11) and an Nd:YAG laser (Continuum surelite, 355 nm, 7 ns pulse width) at 355 nm excitation. Emission lifetimes were measured using a streak camera (Hamamatsu C3434) as a detector. Temperature was controlled with a liquid N_2 cryostat (Oxford instruments, model 01200).

X-ray Diffraction Studies. Suitable single crystals of **1-Br**, **2-Br, 2-I·2CH$_3$CN**, **3-I**, **4-Br**, **5-Br**, **6-B**r, **7-Br**, **8-Br**, **9-Br**, and **10-I·2CH$_3$CN** were obtained as described in the preparation section. The selected crystals were mounted onto a thin glass fiber. Measurements were made on a Mercury CCD area detector coupled with a Rigaku AFC-8S diffractometer and on a Mercury CCD area

Table 1. Summary of X-ray Data Collection and Refinement

	1-Br	**2-Br·2CH$_2$Cl$_2$**	**2-I·2CH$_3$CN**	**3-I**	**4-Br**
formula	$C_{46}H_{38}Br_2Cu_2N_2P_2$	$C_{42}H_{38}Br_2Cl_4Cu_2N_2P_2$	$C_{44}H_{40}Cu_2I_2N_4P_2$	$C_{40}H_{34}Cu_2I_2N_2P_2$	$C_{44}H_{36}Br_2Cu_2N_2P_2$
fw	967.67	1061.44	1067.68	985.57	941.63
cryst syst	triclinic	monoclinic	monoclinic	triclinic	triclinic
space group	$P\bar{1}$	$P2_1/n$	$P2_1/n$	$P\bar{1}$	$P\bar{1}$
a (Å)	9.078(3)	8.854(2)	8.968(6)	10.587(4)	8.289(4)
b (Å)	9.282(3)	17.427(4)	18.15(5)	12.396(4)	9.471(5)
c (Å)	13.677(3)	13.507(3)	13.162(8)	15.157(5)	13.98(1)
α (deg)	71.75(1)	90	90	92.921(5)	86.65(5)
β (deg)	66.70(1)	92.458(4)	93.22(2)	104.059(6)	72.77(4)
γ (deg)	86.09(2)	90	90	103.157(3)	64.94(4)
V (mm^{-3})	1003.1(5)	2082.2(8)	2139(6)	1867(1)	947(1)
Z	1	2	2	2	1
T (K)	153	104	153	293	153
ρ_{calcd} (g cm^{-3})	1.602	1.693	1.657	1.753	1.652
μ (mm^{-1})	3.174	3.313	2.548	2.91	3.360
no. of measured reflns	6057	12583	11356	15612	7764
no. of unique reflns	4066	4682	4560	8128	3672
R_{int}	0.019	0.027	0.033	0.028	0.036
no. of obsd reflns ($I > 2\sigma(I)$)	3358	3872	2729	4027	2048
no. of params	320	320	244	433	235
R1[a]	0.041	0.0281	0.0398	0.0361	0.0655
wR2[b]	0.0858	0.0745	0.0729	0.0496	0.1387
GOF[c]	1.085	0.972	1.064	0.825	1.266

	5-Br	**6-Br**	**7-Br**	**8-Br**	**9-Br**	**10-I·2CH$_3$CN**
formula	$C_{44}H_{36}Br_2Cu_2N_2P_2$	$C_{44}H_{36}Br_2Cu_2N_2P_2$	$C_{50}H_{50}Br_2Cu_2N_4P_2$	$C_{60}H_{48}Br_2Cu_2N_2O_2P_2$	$C_{60}H_{48}Br_2Cu_2N_2O_2P_2$	$C_{44}H_{46}Cu_2I_2N_4P_2$
fw	941.63	941.63	1055.82	1177.9	1177.9	1073.72
cryst syst	triclinic	monoclinic	triclinic	triclinic	monoclinic	monoclinic
space group	$P\bar{1}$	$P2_1/a$	$P\bar{1}$	$P\bar{1}$	$P2_1$	$P2_1/n$
a (Å)	15.269(2)	15.05(1)	10.074(5)	8.210(2)	9.269(3)	9.134(3)
b (Å)	15.255(2)	9.701(6)	14.565(6)	12.632(3)	25.572(7)	17.883(5)
c (Å)	19.038(2)	27.03(3)	17.902(6)	13.944(3)	11.738(4)	13.321(4)
α (deg)	74.781(7)	90	65.15(2)	65.776(9)	90	90
β (deg)	71.636(6)	98.56(2)	83.19(3)	77.72(1)	110.225(6)	90.338(4)
γ (deg)	69.557(6)	90	87.93(3)	83.80(1)	90	90
V (mm^{-3})	3885.1(8)	3902(6)	2366(1)	1288.1(5)	2610(1)	2175(1)
Z	4	4	2	1	2	2
T (K)	153	253	153	153	153	153.1
ρ_{calcd} (g cm^{-3})	1.61	1.603	1.482	1.518	1.498	1.639
μ (mm^{-1})	3.275	3.261	2.698	2.489	2.456	2.506
no. of measured reflns	23719	24780	14278	7834	15596	12467
no. of unique reflns	15868	9344	9597	5248	5712	4733
R_{int}	0.024	0.031	0.047	0.018	0.050	0.020
no. of obsd reflns ($I > 2\sigma(I)$)	12931	7507	6465	4281	4270	4468
no. of params	937	469	541	316	631	324
R1[a]	0.0382	0.0653	0.082	0.0358	0.0388	0.0277
wR2[b]	0.0879	0.1467	0.1889	0.0811	0.0768	0.0916
GOF[c]	1.061	1.409	1.776	1.036	0.811	1.417

[a] $R1 = \sum||F_o| - |F_c||/\sum|F_o|$. [b] $wR2 = \{\sum[w(F_o^2 - F_c^2)^2]/\sum[w(F_o^2)^2]\}^{1/2}$ with $w = \{\sigma^2(F_o^2) + [x(\max(F_o^2,0) + 2F_c^2)/3]^2\}^{-1}$. [c] $GOF = ((\sum(|F_o| - |F_c|)^2)/(N_o - N_v))^{1/2}$ with N_o = no. of obsd reflns and N_v = no. of params.

detector coupled with a Rigaku AFC-7R diffractometer with graphite-monochromated Mo Kα radiation (0.7107 Å). Final cell parameters were obtained from a least-squares analysis of reflections with $I > 10\sigma(I)$. Space group determinations were made on the basis of systematic absences, a statistical analysis of intensity distribution, and the successful solution and refinement of the structures. Data were collected and processed using Crystal Clear.[15] An empirical absorption correction resulted in acceptable transmission factors. The data were corrected for Lorentz and polarization factors.

All the calculations were carried out on a Silicon Graphics O2 computer system using TEXSAN.[16] The structures were solved by direct methods, and were expanded using Fourier and difference Fourier techniques. Because of the problem of crystal size and quality, the R and GOF values are relatively high for **7-Br**, although the basic structural features of the complex have been clearly determined. Details of crystal parameters and structure refinements are given in Table 1. Selected bond lengths and angles are shown in Table S1. Interatomic distances around Cu atoms are listed in Table S2.

Computational Methods. All of the molecular orbital calculations were performed with the Gaussian 03 program[17] at the B3LYP[18] level using a 6-31G**[19] basis set. The energy levels were calculated for the optimized free and protonated *N*-heteroaromatic. The single-point DFT and TD-DFT calculations were carried out for model compound $[Cu_2Br_2(PH_3)_2(py)_2]$. The model compound was assumed to have an idealized C_{2h} structure, with averaged atomic distances and angles found in $[Cu_2Br_2(PPh_3)_2(py)_2]$.[20] The atomic parameters used for the calculation are shown in Table S3.

(15) *Crystal Clear*; Rigaku Corporation: Tokyo, 1999.
(16) *teXsan* version 1.11; Molecular Structure Corporation: The Woodlands, TX, 2000.

Results and Discussion

Synthesis. Fourteen complexes with the general formula $[\{Cu_2(\mu\text{-}X)_2(PPh_3)_2\}(L)_n]$ were synthesized using nine *N*-heteroaromatic ligands and one nonaromatic ligand, piperazine. As described in the next section in detail, the X-ray structural analyses revealed that all the complexes have $\{Cu_2(\mu\text{-}X)_2\}$ structural units. When the *N*-heterocyclic ligand (L) is a bidentate bridging ligand, an extended chain structure is formed. On the other hand, when L is a monodentate ligand, the complex is of a discrete molecular type.

The reactions of Cu(I)−halide with *N*-heteroaromatic ligands have been known to afford compounds with a variety of structural types: monomer, oligomeric $\{Cu_nX_n\}$ units, 1D chain, stair-step polymers, and 2D sheet structures, depending on the choice of solvent system and reaction ratios.[12] This is due to the geometric flexibility of Cu(I) and halide ions. Hitherto, a rational synthetic approach to a specific oligomeric Cu(I)−halide core structure such as $Cu_2(\mu_2\text{-}X)_2$ and $Cu_4(\mu_3\text{-}X)_4$ has not been established.

To restrict the structural types of the products, we chose soft bulky PPh_3 as an ancillary ligand, as it is expected to coordinate to the soft Cu(I) ion more strongly than *N*-heteroaromatic ligands, and its bulkiness may suppress the higher degree of aggregation. This approach enabled us to successfully prepare a series of complexes containing $\{Cu_2(\mu\text{-}X)_2\}$ units with six bidentate *N*-heteroaromatic ligands and nonaromatic piperazine, by the direct mixing of the constituent chemical species.

As the compounds containing bidentate ligands are insoluble in usual organic solvents because of their infinite linear chain structure (vide infra), the purification of the product was practically impossible once the products were obtained. To obtain pure crystalline products, it was necessary to carefully control the concentration of the reactants in the solution at the optimum ratio. If an inappropriately concentrated solution was used, the reaction mixture afforded only powder material. Even if the elemental analyses provided the expected values for these powder materials, structural ambiguities remained because of possible structural isomers.[10f,12b] Only pure crystalline products were used for measurements.[21]

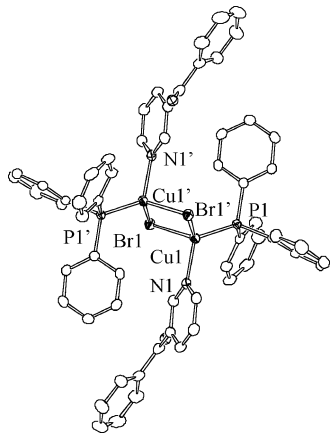

Figure 1. ORTEP drawing of discrete complex **8-Br** with ellipsoids at the 50% probability level. Hydrogen atoms are omitted for clarity. Symmetry operation′: $-x, -y, -z$.

The molecular complexes with monodentate ligands **7-Br**, **8-Br**, and **9-Br** were successfully synthesized by ligand substitution of the acetonitrile complex $[Cu_2(\mu\text{-}Br)_2(PPh_3)_2(CH_3CN)_2]$ in dichloromethane. The yields are acceptable for **8-Br** and **9-Br**, thereby indicating that the substitution reaction is an effective way to prepare the dimeric complex with the $\{Cu_2(\mu\text{-}Br)_2(PPh_3)_2\}$ moiety. The low yield of **7-Br** does not indicate the incomplete progress of the substitution reaction; however, the low yield can possibly be attributed to the relative instability of **7-Br** to oxidation, because a blue Cu(II) complex was obtained under the preparation conditions. Unfortunately, our efforts to prepare the corresponding iodide complex $[Cu_2(\mu\text{-}I)_2(PPh_3)_2(CH_3CN)_2]$ were unsuccessful. Studies to prepare the molecular iodide analogues are in progress at this laboratory.

The preparations of four complexes (**1-I**,[13] **3-I**,[22] **3-Br**,[22] and **6-Br**[22]) have been published during the course of our study. However, the synthetic procedure for bulk samples and single crystals differed in these reports. The preparation of these compounds by our methods directly afforded single crystals from the reaction mixture.

Structures of $[\{Cu_2X_2(PPh_3)_2\}(L)_n]$ (n = 1, 2) Complexes. (a) Discrete Complexes. The structures of discrete complexes **7-Br**, **8-Br**, and **9-Br** have the same features as those reported previously for analogous dimeric complexes $[Cu_2Br_2(PPh_3)_2L_2]$ (L = pyridine,[20] 4-cyanopyridine,[20] quinoline,[23] and piperidine[24]). Figure 1 shows the crystal structure of **8-Br**.

The complex has a $\{Cu_2(\mu\text{-}Br)_2\}$ rhombus as a structural unit that has one PPh_3 and one 3-bzpy ligand coordinating to each Cu atom. The coordination geometry around the Cu

(17) Frisch, M. J.; Trucks, G. W.; Schlegel, H. B.; Scuseria, G. E.; Robb, M. A.; Cheeseman, J. R.; Montgomery, J. A., Jr.; Vreven, T.; Kudin, K. N.; Burant, J. C.; Millam, J. M.; Iyengar, S. S.; Tomasi, J.; Barone, V.; Mennucci, B.; Cossi, M.; Scalmani, G.; Rega, N.; Petersson, G. A.; Nakatsuji, H.; Hada, M.; Ehara, M.; Toyota, K.; Fukuda, R.; Hasegawa, J.; Ishida, M.; Nakajima, T.; Honda, Y.; Kitao, O.; Nakai, H.; Klene, M.; Li, X.; Knox, J. E.; Hratchian, H. P.; Cross, J. B.; Bakken, V.; Adamo, C.; Jaramillo, J.; Gomperts, R.; Stratmann, R. E.; Yazyev, O.; Austin, A. J.; Cammi, R.; Pomelli, C.; Ochterski, J. W.; Ayala, P. Y.; Morokuma, K.; Voth, G. A.; Salvador, P.; Dannenberg, J. J.; Zakrzewski, V. G.; Dapprich, S.; Daniels, A. D.; Strain, M. C.; Farkas, O.; Malick, D. K.; Rabuck, A. D.; Raghavachari, K.; Foresman, J. B.; Ortiz, J. V.; Cui, Q.; Baboul, A. G.; Clifford, S.; Cioslowski, J.; Stefanov, B. B.; Liu, G.; Liashenko, A.; Piskorz, P.; Komaromi, I.; Martin, R. L.; Fox, D. J.; Keith, T.; Al-Laham, M. A.; Peng, C. Y.; Nanayakkara, A.; Challacombe, M.; Gill, P. M. W.; Johnson, B.; Chen, W.; Wong, M. W.; Gonzalez, C.; Pople, J. A. *Gaussian 03*, revision C.02; Gaussian, Inc.: Wallingford, CT, 2004.
(18) (a) Becke, A. D. *J. Chem. Phys.* **1993**, *98*, 5648−5652. (b) Becke, A. D. *Phys. Rev. A* **1988**, *38*, 3098−3100. (c) Lee, C.; Yang, W.; Parr, R. G. *Phys. Rev. B* **1988**, *37*, 785−789.
(19) Hariharan, P. C.; Pople, J. A. *Mol. Phys.* **1974**, *27*, 209.
(20) Engelhardt, L. M.; Healy, P. C.; Kildea, J. D.; White, A. H. *Aust. J. Chem.* **1989**, *42*, 913.
(21) Though the crystal structures of **1-I** and **3-Br** have been reported, we confirmed the structures of our samples by X-ray analysis. They showed results identical to those previously reported.
(22) Maeyer, J. T.; Johnson, T. J.; Smith, A. K.; Borne, B. D.; Pike, R. D.; Pennington, W. T.; Krawiec, M.; Rheingold, A. L. *Polyhedron* **2003**, 22, 419−431.
(23) Jin, Q.-H.; Long, D.-L.; Wang, Y.-X.; Xin, X.-Q. *Acta Crystallogr., Sect. C* **1998**, *54*, 948.
(24) Bowmaker, G. A.; Hanna, J. V.; Hart, R. D.; Healy, P. C.; White, A. H. *J. Chem. Soc., Dalton Trans.* **1994**, 2621.

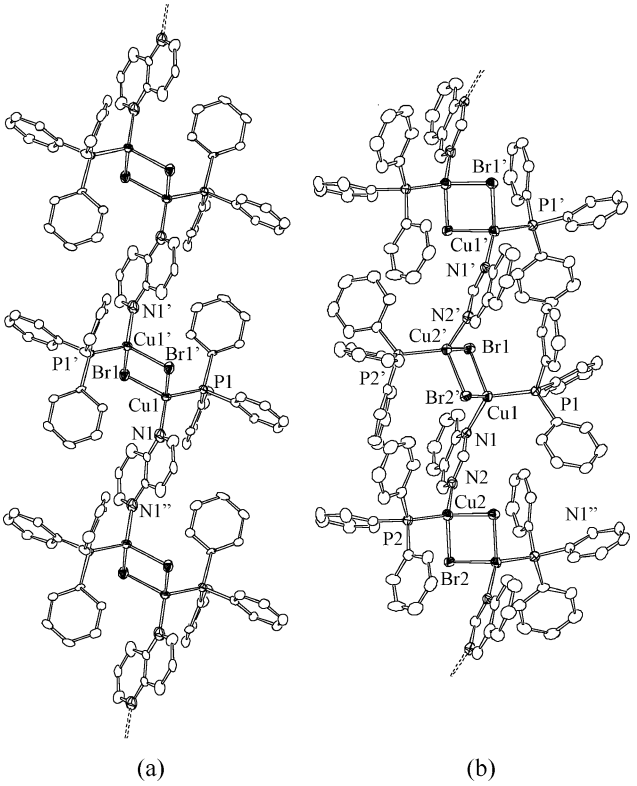

Figure 2. ORTEP drawing of linear chain complexes with ellipsoids at the 50% probability level. Hydrogen atoms are omitted for clarity. (a) **4-Br** symmetry operation′: $-x, -y, -z$. (b) **5-Br** symmetry operation′: $^1/_2 + x$, $^1/_2 - y$, z.

atom is tetrahedral considering one N atom of 3-bzpy, one P atom of PPh_3, and two Br^- ions. The $\{Cu_2Br_2\}$ unit is planar, with its crystallographic inversion center coinciding with its midpoint. The structures of **7-Br** and **9-Br** are similar to that of **8-Br**; however, it is noteworthy that their molecular structures do not have inversion centers, although their bond distances and angles showed virtual C_i symmetry. The small deviations bring two *N*-heteroaromatic ligands that are inequivalent with respect to **7-Br** and **9-Br**, which is interestingly reflected in dual emission lifetimes (vide infra).

(b) Polymeric Complexes. The bidentate ligands employed here have two nitrogen donors located in a manner so as to enable the interunit (-$\{Cu_2X_2\}$-) bridging coordination rather than a chelate or intraunit bridging coordination. Such ligands afford linear chain complexes with the bidentate ligands acting as a bridge between the two $\{Cu_2X_2\}$ units. The linear chain structure appears to be the common motif for $\{Cu_2X_2\}$ complexes with PR_3 and the bidentate *N*-heteroaromatic ligands.[12a,b,13,14]

Figure 2a shows the crystal structure of **4-Br**, in which an alternate arrangement of rhombic $\{Cu_2Br_2\}$ units and bridging 1,5-nap ligands form the 1-dimensional chain structure. In the structure of **4-Br**, two crystallographic inversion centers are superimposed on the midpoint of the $\{Cu_2Br_2\}$ unit and on the center of the 1,5-nap ligand. The complexes with other centric ligands (**1-Br** and **2-Br**) show similar chain structures. In these complexes, all the dimeric units in the chain are structurally equivalent. When acentric *N*-heteroaromatic ligands such as pym, 1,6-nap, and quina

Table 2. Emission Maxima (λ^{em}_{max}) and Lifetimes (τ^{em})of the Complexes

	λmax (nm)		lifetime (μs)	
	rt	80 K	rt	80 K
X = Br				
1-Br (bpy)	595	614	3.1(1)	16(1)
2-Br (pyz)[a]	707	780	0.42(1)/0.06(2)	3.2(3)/1.11(1)
3-Br (pym)	579	599	2.9(1)	29(2)
4-Br (1,5-nap)	616	642	5.6(1)	52(1)
5-Br (1,6-nap)[b]	633	655	7.6(6)/0.69(2)	23(1)/4.4(1)
6-Br (quina)	644	668	0.60(1)	10 (1)
7-Br (dmap)[b]	450	468	7.5(3)/2.3(1)	430(10)/48(3)
8-Br (3-bzpy)	579	599	0.75(1)	9.0(1)
9-Br (4-bzpy)[b]	689	730	0.16(1)/0.039(2)	4.0(1)/0.096(3)
X = I				
1-I (bpy)[c]	542	542	4.0(1)	67(1)
2-I (pyz)[a]	648	671	1.7(1)	31(1)/5.9(3)
3-I (pym)	562	576	2.7(1)	37(1)

[a] Main components of decay curves were fit with a double-exponential function for comparison with the other complexes. [b] Decay curves were fit with a double-exponential function. [c] λ^{em}_{max} for **1-I** at room temperature has been reported to be 535 nm. See ref 13.

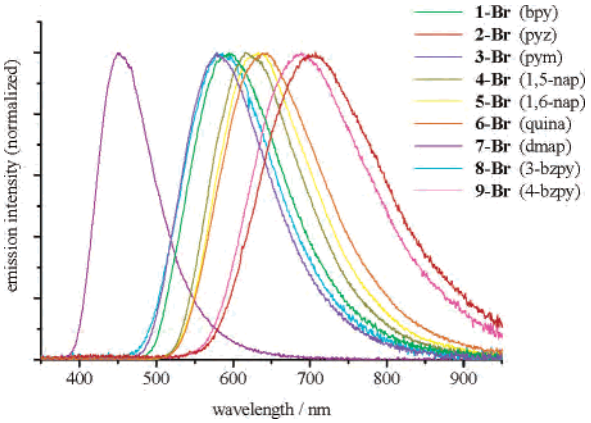

Figure 3. Emission spectra of bromide complexes **1-Br**−**9-Br** at room temperature.

are used, the resulting linear chain structures are distorted (Figure 2b). As the structure of **5-Br** (Figure 2b) manifests itself, the neighboring $\{Cu_2Br_2\}$ units get oriented in different directions along the chain, and are structurally nonequivalent. Because of the skewed direction of the nitrogen lone pairs in acentric ligands, neighboring $\{Cu_2Br_2\}$ rhombuses are compelled to assume an oblique arrangement. The planarity of $\{Cu_2Br_2\}$ units is intact for all complexes. The iodide complexes are obtained as isostructural crystals corresponding to the bromide complexes.

Emission Properties. (a) Emission Spectra and Lifetimes. A series of complexes prepared in this study, except for the piperazine complexes **10-I** and **10-Br**, show strong emission in the solid state at room temperature.[25] The emission maxima (λ^{em}_{max}) and the lifetimes at room temperature and at 80 K are shown in Table 2. Figure 3 shows the emission spectra of the bromide complexes at room temperature.

The emission maxima of the complexes cover a wide range, from 450 to 740 nm depending on the *N*-heteroaro-

(25) Using preliminary measurements with an integrating sphere at room temperature, we determined the quantum yields of **1-Br** and **1-I** to be 0.18 and 0.23, respectively.

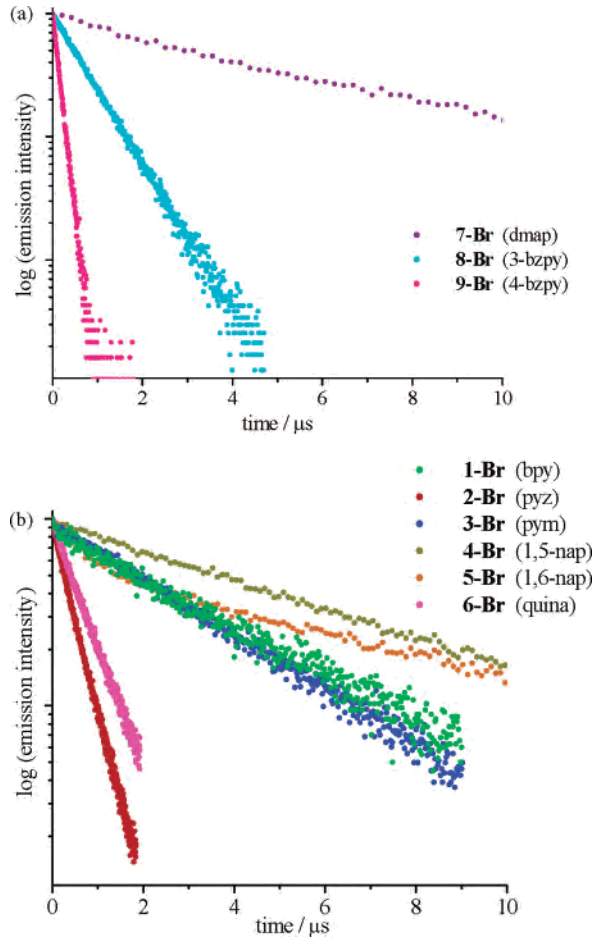

Figure 4. Emission decay of bromide complexes: (a) discrete complexes **7-Br**−**9-Br**, (b) linear chain complexes **1-Br**−**6-Br**.

matic ligands. The emissions of the iodide complexes are higher in energy than those of corresponding bromide complexes by 520−1900 cm^{-1} (Table 2). Figure 4 shows the emission decay curves of the bromide complexes at room temperature. The emission lifetimes are in the microsecond range, indicating phosphorescence emissions from the triplet excited state. At low temperatures, the lifetimes become longer and the emission maxima shift to a higher-energy region by 430−1300 cm^{-1}.[26] The conventional measurements of absorption and excitation spectra of the present complexes in solution were not possible because of the complexes' insoluble natures and their possible decomposition in the solution if dissolved.[27] Even for those having absorption near the UV region, the absorption and excitation spectra in the solid state did not afford clear information because of the scattered light. Nevertheless, the color of the complexes has a good correlation with their emission bands (Table S4). The only complex that provided meaningful information is [{$Cu_2(\mu$-$I_2)(PPh_3)$}$_2$(pyz)], in that both spectra showed a broad band centered around 500 nm (Figure S1).

(b) Structures and Emission Decay Patterns. As shown in Figure 4, several complexes showed a deviation from single-exponential decay. It is interesting to note that the behavior is correlated with the crystal structures. Complexes showing single-exponential decay are **1-Br**, **1-I**, **3-Br**, **3-I**, **4-Br**, **6-Br**, and **8-Br**. The crystals for all these complexes contain one crystallographically independent *N*-heteroaromatic ligand. The pym complex **3-Br** and **3-I** and the quinazoline complex **6-Br** showed single-exponential decay, although the complexes contain two crystallographically independent Cu(I) ions in the crystals. On the other hand, complexes **5-Br**, **7-Br**, and **9-Br**, which show a deviation from single-exponential decay, have two crystallographically independent *N*-heteroaromatic ligands. The results suggest that each {Cu(I)-L} (L = *N*-heteroaromatic ligands) unit independently behaves as an emission center in the case of discrete complexes with monodentate ligands. The results also imply that the {Cu(I)-L-Cu(I)} units play a major role in emission in the case of the polymeric complexes with bidentate *N*-heteroaromatic ligands.[28] The deviation from single-exponential decay of **2-Br** and **2-I** that have one crystallographically independent pyz may be explained by the release of labile crystal solvents, resulting in structural deviation from those determined by X-ray analysis.[29]

(c) Relationship between the Reduction Potential of the Ligands and Emission Energies of the Complexes. The emission energies of a series of the dicopper complexes are strongly affected by the *N*-heteroaromatic ligands (L). The emission was not observed for complexes with the non-π-type ligand pip. Thus, the charge-transfer excited state to π^* orbitals of *N*-heteroaromatic ligands is assumed to be the origin of the emission in the series of complexes.

In previous papers, several possible lowest excited states have been suggested for the emissive Cu(I)−halide complexes.[9b] These include metal-centered (d → s), MLCT, XLCT, intraligand, and cluster-centered (CC) excited states. The emission of the chloride complex [{$Cu_2(\mu$-$Cl)_2(PPh_3)_2$}-(pyz)] has been assigned to the Cu(I)-to-pyrazine MLCT excited state on the basis of resonance Raman spectroscopy.[14] Ford et al. reported the emission of a series of py complexes [($Cu_2(\mu$-$X)_2(PPh_3)_2$)$(py)_2$] (X = I, Br, Cl), and pointed out the possibility of the XLCT excited state.[9a] They also studied the emission of the {$Cu_2(\mu$-$I)_2$} complexes without PPh_3,[10d] and reported that the emission of [$Cu_2(\mu$-$I)_2$(tetraethylethylenediamine)$_2$] is attributed to a CC transition and that the emission of [$Cu_2(\mu$-$I)_2(py)_4$] is mainly attributed to both CC transition and XLCT.[10b] Both these transitions are unlikely in our complexes, because no clear correlation between Cu−Cu distances and emission maxima was observed and also because the effects of bridging halides were smaller than those of *N*-heteroaromatic ligands.

(26) **1-I** did not show the bathochromic shift, but showed the slightly structured spectrum at 80 K. The single-exponential decay of **1-I** at 80 K ruled out the appearance of a new excited state.

(27) Molecular complexes are soluble to organic solvents such as CH_2Cl_2, $CHCl_3$, and acetonitrile. However, the extinction coefficients obtained by the UV−vis absorption measurements did not obey the Lambert−Beer law, showing the degradation of the complexes in the solvent. NMR spectra show the signals corresponding to the free PPh_3 and *N*-heteroaromatic ligands, which also indicate the weak binding and fluctuation of the ligands in solution.

(28) From this point of view, the structure can be described as the linear chain composed of {Cu(I)-L-Cu(I)} and bridging halide ligands.

(29) The powder X-ray diffraction pattern of the **2-Br** samples showed the broad signals slightly deviated from those expected for the structures determined by the single-crystal structure analysis.

Table 3. Reduction Potentials of *N*-Heteroaromatic Ligands (L) and λ^{em}_{max} of $[Cu_2Br_2(PPh_3)_2(L)_n]$

L	*n*	redox potential (V)[a]	λ^{em}_{max} (nm)
bpy	2	−1.84	595
pyz	2	−2.10	707
pym	2	−2.35	579
1,5-nap	2	−1.82	616
1,6-nap	2	−1.79	633
quina	2	−1.74	644
4-bzpy	1	−1.46	686
3-bzpy	1	−1.60	579
py	1	−2.76[b]	487[c]

[a] In acetonitrile, vs Ag|AgCl. [b] Ref 31. [c] Ref 9a.

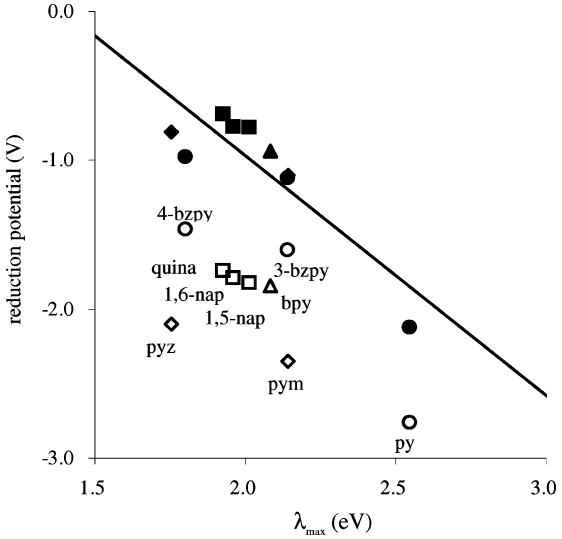

Figure 5. Emission maxima and reduction potentials of *N*-heteroaromatic ligands. Filled symbols show the values corrected for the protonation (see text). The slope of the best fitting line is −1.6(3) with a correlation coefficient of −0.87 and a reduced χ^2 of 0.053.

We further discuss the emissive excited state in favor of the MLCT transition. The linear correlation between the MLCT transition energies and reduction potentials of the ligands for homologous complexes has been assumed for localized CT models.[30] Table 3 lists the reduction potential of the ligands and the λ_{max} of the complexes.

The emission energy increases in the order of the reduction potentials of the ligands in the case of discrete complexes $[(Cu_2Br_2(PPh_3)_2)(L)_2]$ (L = dmap, py, 3-bzpy, 4-bzpy). However, the correlation becomes obscured when the chain-type complexes are included (Figure 5).

We ascribed this inconsistency to the use of the reduction potentials of free ligands themselves instead of the coordinated ligands. The π^* orbitals of *N*-heteroaromatic ligands should be stabilized by the coordination to the Lewis acid, Cu(I). Because of their insolubility, the direct measurement of the reduction potentials in the complexes was not possible. To estimate the extent of stabilization of the π^* energy level on coordination, we calculate the π^* energy level for protonated ligands as the simplest models of Lewis acid complexes (Table 4).[32]

Table 4. Stabilization of LUMO Levels (ΔE) on Protonation (eV)[a]

	first protonation	second protonation	total
bpy	5.19	3.85	9.01
pyz	6.52	6.37	12.89
pym	6.48	6.01	12.49
1,5-nap	5.41	5.03	10.44
1,6-nap	5.48	4.68	10.16
quina	5.47	5.04	10.51
dmap	5.60		5.60
py	6.40		6.40
4-bzpy	4.84		4.84
3-bzpy	4.83		4.83

[a] Stabilization of LUMO levels in protonated forms is estimated as $\Delta E = -(E_{LUMO}(LH^+) - E_{LUMO}(L))$.

As expected, the π^* orbitals of the bidentate ligands are more stabilized by protonation, as two protons are attached to the ligands. Among the bidentate ligands, the total stabilization energies of the π^* orbitals are significantly different by as much as 3.85 V, as exemplified by the difference between bpy (9.04 V) and pyz (12.89 V). This result is reasonable, because the π^* orbital of pyz is confined on one six-membered ring, making the π^* orbital of pyz more sensitive to protonation than that of bpy.[33] We assume that the stabilization energy of the π^* orbital by the coordination is linearly correlated with that by the protonation in terms of these stabilization energies given by the formula $E(\pi^*) = E(\text{red}) + aE(\text{stabilization})$. When a is assumed to be 0.1, the calculated energy and the emission energy showed good linear correlation (Figure 5, filled symbols). Although the strict estimation of emission energies needs more delicate consideration for orbital energies in ground and excited states, the linear correlation in Figure 5 shows that qualitative prediction is possible, at least in our complexes, using the redox potential and a simple energy calculation for free and protonated ligands.

(d) Properties of HOMO and LUMO. From the aforementioned discussion, the π^* orbitals of *N*-heteroaromatic ligands are clearly related to the emissive excited state in a series of the dicopper complexes. In that context, the available MO calculations of $\{Cu_2(\mu\text{-}X)_2\}$ complexes $[Cu_2I_2(NH_3)_4]$,[10b] $[Cu_2I_2(py)_4]$,[10b] and $[Cu_2I_2(PH_3)_4]$[34] are highly relevant. For amine and phosphine model complexes, the orbitals around frontier orbital levels have been reported[10b,34] to mainly possess copper and iodine characters, showing that the absorption and emission bands in the UV−vis region can be ascribed to the transitions within cluster units. For the pyridine model complex, py π characters appear in the LUMO (lowest unoccupied molecular orbital) in addition to copper and iodine characters. Thus the transitions have more MLCT character in the pyridine complex.[10b]

(30) (a) Juris, A.; Balzani, V.; Barigelletti, F.; Campagna, S.; Belser, P.; Von Zelewsky, A. *Coord. Chem. Rev.* **1988**, *84*, 85−277. (b) Juris, A.; Campagna, S.; Balzani, V.; Gremaud, G. *Inorg. Chem.* **1988**, *27*, 3652−3655.

(31) Tabner, B. J.; Yandle, J. R. *J. Chem. Soc. A* **1968**, 381−388.

(32) Because Cu(I) is a d^{10} spherical ion, we assumed that the effects of coordination to Cu(I) should be estimated by the protonated compounds at the first approximation.

(33) The stabilization energies for the first protonation differ little (5.19 and 6.52 V). However, the stabilization energy of bpy for the second protonation is much smaller than that of pyz (3.85 and 6.37 V, respectively). The stabilization on first protonation is similar for bpy and pyz because the LUMO orbital is mainly localized on the protonated pyridine ring, as the $(bpyH)^+$ is no longer symmetrical.

(34) Aslanidis, P.; Cox, P. J.; Divanidis, S.; Tsipis, A. C. *Inorg. Chem.* **2002**, *41*, 6875−6896.

Table 5. Calculated Energies and Components of MO for $[Cu_2Br_2(PH_3)_2(py)_2]$ around Frontier Orbital Levels

MO	energy (eV)	symmetry	Cu	Br	py	PH_3
L + 4	0.68	a_u	0.29	0.00	0.01	0.70
L + 3	−0.57	b_g	0.01	0.00	0.99	0.00
L + 2	−0.58	a_u	0.00	0.00	0.99	0.00
L + 1	−0.85	b_u	0.02	0.00	0.97	0.00
LUMO	−0.85	a_g	0.02	0.01	0.97	0.00
HOMO	−4.35	b_u	0.70	0.23	0.02	0.05
H − 1	−4.62	a_u	0.74	0.23	0.01	0.02
H − 2	−4.71	b_u	0.68	0.19	0.06	0.06
H − 3	−4.74	a_g	0.86	0.02	0.08	0.04
H − 4	−4.96	a_g	0.83	0.04	0.05	0.08
H − 5	−5.05	b_g	0.76	0.23	0.01	0.00

We have carried out the MO calculation on the mixed-ligand bromide model complex $[Cu_2Br_2(PH_3)_2(py)_2]$ by the DTF method on Gaussian 03. The geometry of the model compound was taken from the crystal structure of $[Cu_2Br_2(PPh_3)_2(py)_2]$,[20] and virtual C_{2h} symmetry was assumed. The calculated energy levels around the frontier orbitals are similar to that of the previous iodide−pyridine model complex in that the orbitals are mainly composed of copper, halide, and pyridine orbitals. Table 5 shows the energy and components of each molecular orbital of $[Cu_2Br_2(PH_3)_2(py)_2]$ around the frontier orbital levels.

The HOMO (highest occupied molecular orbital) was mainly composed of Cu-3d and Br-3p orbitals. The other occupied MOs around the HOMO are also mainly composed of Cu-3d and Br-3p orbitals.[35] The LUMO and L+1 to L+3 were essentially py π^* orbitals. When the Cu−Cu distance is short enough, the Cu-4s4p orbitals become the LUMO because of the stabilization by Cu−Cu bonding interaction, as has been previously reported for $[Cu_2I_2(NH_3)_4]$.[10b] However, the long Cu−Cu distance in this system weakened the Cu−Cu interaction leaving the Cu 4s and 4p orbitals at a higher energy. Accordingly, the relatively stable py π^* orbital becomes LUMO in this model.

The lowest-energy transition calculated by the TD-DFT method is mainly composed of a HOMO−LUMO transition (HOMO → LUMO (85%) and HOMO − 3 → LUMO + 1 (8%)). The calculated transition energy was 2.72 eV (456 nm) with an oscillator strength of 0.0029. The calculation on the model complex supports the fact that the emissions of $[Cu_2X_2(PPh_3)_2(L)_n]$ are related to the excited state formed by the charge transfer from the metal d orbital to the π^* orbital of the *N*-heteroaromatic ligand. The mixing of the Br orbitals to occupied MOs around the HOMO shows the addition of XLCT properties to the excited state. The observed satisfactory relationship between reduction potentials of *N*-heteroaromatic ligands and emission energies is explained by the almost pure py π^* properties of the unoccupied orbitals around the LUMO.

(35) We carried out the MO calculation for the corresponding iodide complex that shows results similar to those for the bromide complex. The mixing of iodine and copper AOs around the HOMO was greater than that found in bromide complexes.

Conclusion. A series of Cu(I)−halide complexes with the formula $[\{Cu_2X_2(PPh_3)_2\}(L)_n]$ (L: monodentate, $n = 2$; L: bidentate, $n = 1$) were prepared using nine different *N*-heteroaromatic ligands (L). The emission energy strongly depends on the *N*-heteroaromatic ligands, whereas the effects due to the bridging halide ion and the structural distortions in the $\{Cu_2(\mu\text{-}X)_2\}$ units are less significant. With changes in *N*-heteroaromatic ligands, the emission energies vary significantly over the visible region from red to blue. Easy preparation and tunability of the emission energy of $\{Cu_2(\mu\text{-}X)_2\}$ complexes are useful for the design of emissive materials. The structures of the complexes reveal that the Cu···Cu distances of $\{Cu_2X_2\}$ units tend to be long enough to neglect Cu···Cu direct interactions. Due to the negligible interaction between the two copper atoms, the emission of the present complexes becomes simple; this is in contrast to the temperature-dependent dual emission of related tetranuclear $\{Cu_4I_4L_4\}$ complexes.[9a,10] Although the redox potentials of the present complexes are not measurable, the emission energies were successfully explained by the reduction potentials of the *N*-heteroaromatic ligands that are modified based on the MO calculation for protonated and free ligands. The results provide useful information for the construction of systems with desired emissive properties by selecting the π^* levels of monodentate and bidentate ligands.

Acknowledgment. The authors are indebted to Prof. Kiyoshi Tanaka (Hokkaido University) and Prof. Katsuaki Nobusada (currently at the Institute for Molecular Science) for the calculation. This work was partly supported by a Grant-in-Aid for Young Scientists (B) (17750046) from the Japan Society for the Promotion of Science (JSPS).

Supporting Information Available: The absorption and excitation spectra of **2-I**, selected bond distances and angles of the complexes, atomic parameters of the model complex, interatomic distances around Cu atoms, color and emission maxima of the complexes, and CIF files of the crystals. This material is available free of charge via the Internet at http://pubs.acs.org.

IC0510359